Conformational Analysis and Kinetics of Ring Inversion for Methylene- and Dimethylsilyl-Bridged Dicyclooctatetraene

Stuart W. Staley,*[,‡] Scott A. Vignon,[‡,†] and Bertil Eliasson*[,§]

Contribution from the Departments of Chemistry, Carnegie Mellon University, Pittsburgh, Pennsylvania 15213 and Umeå University, SE-901 87, Umeå, Sweden

staley@andrew.cmu.edu

Received December 26, 2000

Dicyclooctatetraenylmethane (**1**) and dicyclooctatetraenyldimethylsilane (**2**) in THF-d_8 at 272 K exist as mixtures of diastereomers in ratios of 1:0.8 and 1:1, respectively. Nine energy minima (four meso and five racemic conformers) were located for each compound by geometry optimization at the HF/6-31G* level of theory. The effects of torsional strain, steric interactions and dynamic electron correlation were analyzed. The diastereomeric ratios for **1** and **2** were reproduced reasonably well from the total energy calculated for each conformer corrected for its conformational enthalpy and entropy contributions. The ratio of rate constants for bond shift (BS) (k_{BS}(**1**)/k_{BS}(**2**)) is three times greater than the corresponding ratio for ring inversion. This suggests that additional substituent effects, such as π interactions, are operative in the transition state for BS.

Introduction

Ring inversion (RI) and bond shift (BS) (Figure 1) are two fundamental dynamic processes of cyclooctatetraene (COT) that are closely related to each other.[1] In addition to their intrinsic interest, they are important for understanding the role of ring flattening in the "gated" charge transfer (CT) that occurs in bridged dicyclooctatetraenes (Figure 2).[2−5] The bridge could, in principle, affect CT both at the ring flattening and bond equalization ("gating") steps and during the actual transfer of charge (electron and counterion) from one planar COT ring to the other ("intrinsic" CT). The clarification of this issue would allow a better understanding of intrinsic CT, i.e., of the actual charge conduction pathways in these dianions.

The transition structure (TS) for RI in COT is generally described[1b,6] and calculated[7−9] as a planar (D_{4h}) ring with localized π bonds. Recent computational[8] and experimental[10] evidence has confirmed the initial assumption[11] that BS in unsubstituted COT proceeds through a planar bond-equalized (D_{8h}) TS with delocalized π electrons.

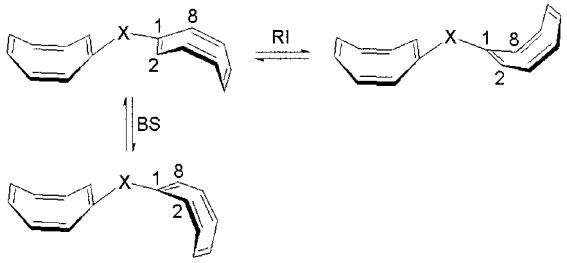

Figure 1. Ring inversion and bond shift in **1** (X = CH_2) and **2** (X = $Si(CH_3)_2$).

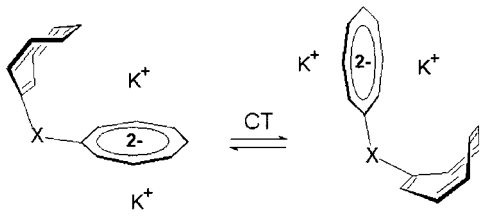

Figure 2. Charge transfer in $\mathbf{1}^{2-}/2K^+$ (X = CH_2) and $\mathbf{2}^{2-}/2K^+$ (X = $Si(CH_3)_2$).

A Hückel molecular orbital (HMO) description of D_{8h} COT shows two degenerate half-occupied frontier MOs or highest occupied (HOMO) and lowest unoccupied (LUMO) MOs. On the basis of this model, the BS TS of COT would be expected to interact more strongly with both donor and acceptor substituents (owing to its low-lying LUMO and high-lying HOMO, respectively) than would the corresponding RI TS, which has localized π bonds.

However, it is well-known that a simple MO model is inadequate for D_{8h} COT because of pseudo Jahn−Teller coupling between energetically similar configurations of the same symmetry.[12] Thus, a large multiconfigurational wave function is required in order to adequately model

‡ Carnegie Mellon University.
† Beckman Scholar, 1999−2000.
§ Umeå University.

(1) (a) Fray, G. I.; Saxton, R. G. *The Chemistry of Cyclo-octatetraene and its Derivatives*; Cambridge: New York, 1978. (b) Paquette, L. A. *Acc. Chem. Res.* **1993**, *26*, 57.
(2) Boman, P.; Eliasson, B. *Acta Chem. Scand.* **1996**, *50*, 816.
(3) Staley, S. W.; Kehlbeck, J. D.; Grimm, R. A.; Sablosky, R. A.; Boman, P.; Eliasson, B. *J. Am. Chem. Soc.* **1998**, *120*, 9793.
(4) Boman, P.; Eliasson, B.; Grimm, R. A.; Martin, G. S.; Strnad, J. T.; Staley, S. W. *J. Am. Chem. Soc.* **1999**, *121*, 1558.
(5) Boman, P.; Eliasson, B.; Grimm, R. A.; Staley, S. W. *J. Chem. Soc., Perkin Trans. 2*, accepted for publication.
(6) Anet, F. A. L.; Bourn, A. J. R.; Lin, Y. S. *J. Am. Chem. Soc.* **1964**, *86*, 3576.
(7) Trindle, C.; Wolfskill, T. A. *J. Org. Chem.* **1991**, *56*, 5426.
(8) Hrovat, D. A.; Borden, W. T. *J. Am. Chem. Soc.* **1992**, *114*, 5879.
(9) Andrés, J. L.; Castaño, O.; Morreale, A.; Palmeiro, R.; Gomperts, R. *J. Chem. Phys.* **1998**, *108*, 203.
(10) Wenthold, P. G.; Hrovat, D. A.; Borden, W. T.; Lineberger, W. C. *Science* **1996**, *272*, 1456.
(11) Anet, F. A. L. *J. Am. Chem. Soc.* **1962**, *84*, 671.
(12) Koseki, S.; Toyota, A. *J. Phys. Chem. A* **1997**, *101*, 5712 and references cited therein.

10.1021/jo001793a CCC: $20.00
Published on Web 05/02/2001

Table 1. Kinetic Data for Ring Inversion and Bond Shift in Monosubstituted Cyclooctatetraenes at 273 K

substituent	k_{RI} (s^{-1})	$\Delta G^{\ddagger}_{RI}$[a]	k_{BS} (s^{-1})	$\Delta G^{\ddagger}_{BS}$[a]
ethyl[b]	180	13.1 ± 0.1	2.7	15.4 ± 0.1
ethoxy[c]	604	12.5	0.9	16.0
isopropoxy[c]	361	12.7	1.9	15.6
isopropoxy[d]	154	13.2		

[a] In kcal mol^{-1}. [b] In THF-d_8; ref 16. [c] Ref 17. [d] Ref 18; extrapolated from an Arrhenius plot over the range 223−261 K.

this species.[8−10,12,13] Nevertheless, the effect of donors and acceptors on the BS relative to the RI TS is a question of considerable interest. Does a simple HMO model qualitatively predict substituent effects on dynamic processes in COT, or are different results obtained owing to the contribution of configuration interaction?

The literature provides neither an extensive nor a reliable guide to answering this question. There are only a few cases where the kinetics of both RI and BS have been studied for the same compounds and most of these have been for carbon-substituted COTs.[3,14,15] We recently determined the rate constants for both RI and BS in ethylCOT.[16] Comparison of these values with the corresponding values for the sterically similar ethoxyCOT[17] (Table 1) suggests that the latter compound undergoes RI *faster* but BS *slower* than ethylCOT (by factors of 3.4 and 0.3, respectively). Comparison of ethylCOT with isopropoxyCOT[17] (which should also have similar steric effects) gives factors of 2.0 and 0.7, respectively. However, Stevenson et al.,[18] by working at 400 MHz ^{1}H NMR frequency compared to the 60 MHz originally employed by Oth,[17] obtained a value of k_{RI} for isopropoxyCOT that is only 0.9 (instead of 2.0) times the corresponding value for ethylCOT at 273 K. From these values, one could conclude that the differential substituent effects of ethyl and isopropoxy are the same (within experimental uncertainty) on RI and BS. However, such a conclusion is contingent on the acceptance of a value of k_{BS} for isopropoxyCOT obtained at 60 MHz.[17]

In the foregoing, an ethyl group, which is a σ donor, is compared with an alkoxy group, which is a σ acceptor and π donor. We have recently analyzed how σ acceptors reduce the barrier for ring flattening and bond shift in COT.[19−21] According to the Walsh/Bent model, the substituted carbon (C_1) contributes less s character to the exocyclic bond as the substituent becomes more electronegative.[22,23] This favors the planar ring (the RI or BS TS) over ground-state COT since the exocyclic orbital at C_1 in the planar ring has less s character. (The CCC bond angle in COT increases from 126.7° in ground state (D_{2d}) COT[24] to 135° in planar (D_{4h} or D_{8h}) COT.) The same conclusion can be reached on the basis of a simple valence-shell electron-pair repulsion (VSEPR) model.[25] Change of substituent electronegativity should affect the σ bonds of the RI and BS TSs equally. Thus, a differential effect between ethyl and ethoxy (Table 1), if real, is probably due to a π effect of the ethoxy group.

Electropositive substituents (e.g., Si, Ge and Sn) have an effect that is opposite to that of electronegative substituents, i.e., they increase the barrier to ring flattening.[20] This observation, along with the ambiguous results for alkoxy groups discussed above, led us to question whether there is any differential effect of electronegative vs electropositive substituents on RI and BS.

The dipotassium salts of dicyclooctatetraenylmethane (**1**) and dicyclooctatetraenyldimethylsilane (**2**) have recently been the subject of several studies of CT (Figure 2).[2,5] Compounds **1** and **2** are also appropriate for the study of both RI and BS (Figure 1). The CH_2COT group is a weak donor, whereas $Si(CH_3)_2$COT is an acceptor.[26] Since monosubstituted COT is a chiral moiety, **1** and **2** each exist as three stereoisomers, a meso isomer and a pair of enantiomers (racemic isomer). The forward and reverse rate constants for exchange of these diastereomers (k_{1exch} and k_{-1exch}, respectively) and k_{BS} can be determined by ^{13}C NMR spectrometry and used to calculate k_{RI}. We anticipated that the results of this study would help to clarify the role of the gating steps for CT in $\mathbf{1}^{2-}/2K^+$ and $\mathbf{2}^{2-}/2K^+$. This has proven to be the case, as reported below.

Results and Discussion

The ^{13}C NMR spectra of **1** and **2** show only eight signals from olefinic carbons at room temperature. However, when the temperature is reduced to 240 or 263 K, respectively, where RI is slow on the NMR time scale, many peaks separate into pairs of signals corresponding to the meso and racemic isomers. This behavior is illustrated for compound **2** in Figure 3. The ^{1}H NMR integrals show that the diastereomers of **1** exist in a 1:0.8 ratio at 229 K, corresponding to a free energy difference ($\Delta G°_{isom}$) of 0.10 ± 0.05 kcal mol^{-1}. The same value was obtained from the ratio k_{1exch}/k_{-1exch} ($\Delta\Delta G^{\ddagger}_{RI} = \Delta G°_{isom} =$ 0.1 kcal mol^{-1}) at 240 and 229 K, as discussed in the Kinetics section. The diastereomers of **2** exist in a 1:1 ratio at 232 K (Figure 3).

Structures and Energies of Conformers. A careful search of the potential energy surface at the HF/3-21G level and then at the HF/6-31G* level has shown that the meso diastereomers of **1** and **2** have four different conformational minima, while the racemic isomers have five (Tables 2 and 3 and Figures 4 and 5). These minima are primarily distinguished by their torsional angles and are of three types.

In AB-type conformers, the C_1C_2 double bonds of the two COT rings are essentially eclipsed with the CH bonds (designated CH_A and CH_B) of the bridge. The meso isomer of this type is designated *meso*-AB′, where the absence or presence of a prime indicates that the other COT ring is endo (above the "tub") or exo (outside the "tub"), respectively, with respect to the designated COT ring.

(13) (a) Karadakov, P. B.; Gerratt, J.; Cooper, D. L.; Raimondi, M. *J. Phys. Chem.* **1995**, *99*, 10186. (b) Glukhovtsev, M. N.; Bach, R. D.; Laiter, S. *J. Mol. Struct.* (*THEOCHEM*) **1997**, *417*, 123.
(14) Anderson, J. E.; Kirsch, P. A. *J. Chem. Soc., Perkin Trans. 2* **1992**, 1951.
(15) Staley, S. W.; Kehlbeck, J. D. *Org. Lett.* **1999**, *1*, 565.
(16) Grimm, R. A., Ph.D. Thesis, Carnegie Mellon University, 1997.
(17) Oth, J. F. M. *Pure Appl. Chem.* **1971**, *25*, 573.
(18) Stevenson, C. D.; Brown, E. C.; Hrovat, D. A.; Borden, W. T. *J. Am. Chem. Soc.* **1998**, *120*, 8864.
(19) Staley, S. W.; Grimm, R. A.; Martin, G. S.; Sablosky, R. A. *Tetrahedron* **1997**, *53*, 10093.
(20) Staley, S. W.; Grimm, R. A.; Sablosky, R. A. *J. Am. Chem. Soc.* **1998**, *120*, 3671.
(21) Peterson, M. L.; Staley, S. W. *Struct. Chem.* **1998**, *9*, 305.
(22) (a) Walsh, A. D. *Discuss. Faraday Soc.* **1947**, *2*, 18. (b) Bent, H. A. *Chem. Rev.* **1961**, *61*, 275.
(23) Domenicano, A. *Methods Stereochem. Anal.* **1988**, *10*, 281.
(24) Claus, K. H.; Krüger, C. *Acta Crystallogr. C* **1988**, *44*, 1632.
(25) Gillespie, R. J. *Angew. Chem., Int. Ed. Engl.* **1967**, *6*, 819; *J. Chem. Educ.* **1970**, *47*, 18.
(26) Echegoyen, L.; Maldonado, R.; Nieves, J.; Alegria, A. *J. Am. Chem. Soc.* **1984**, *106*, 7692.

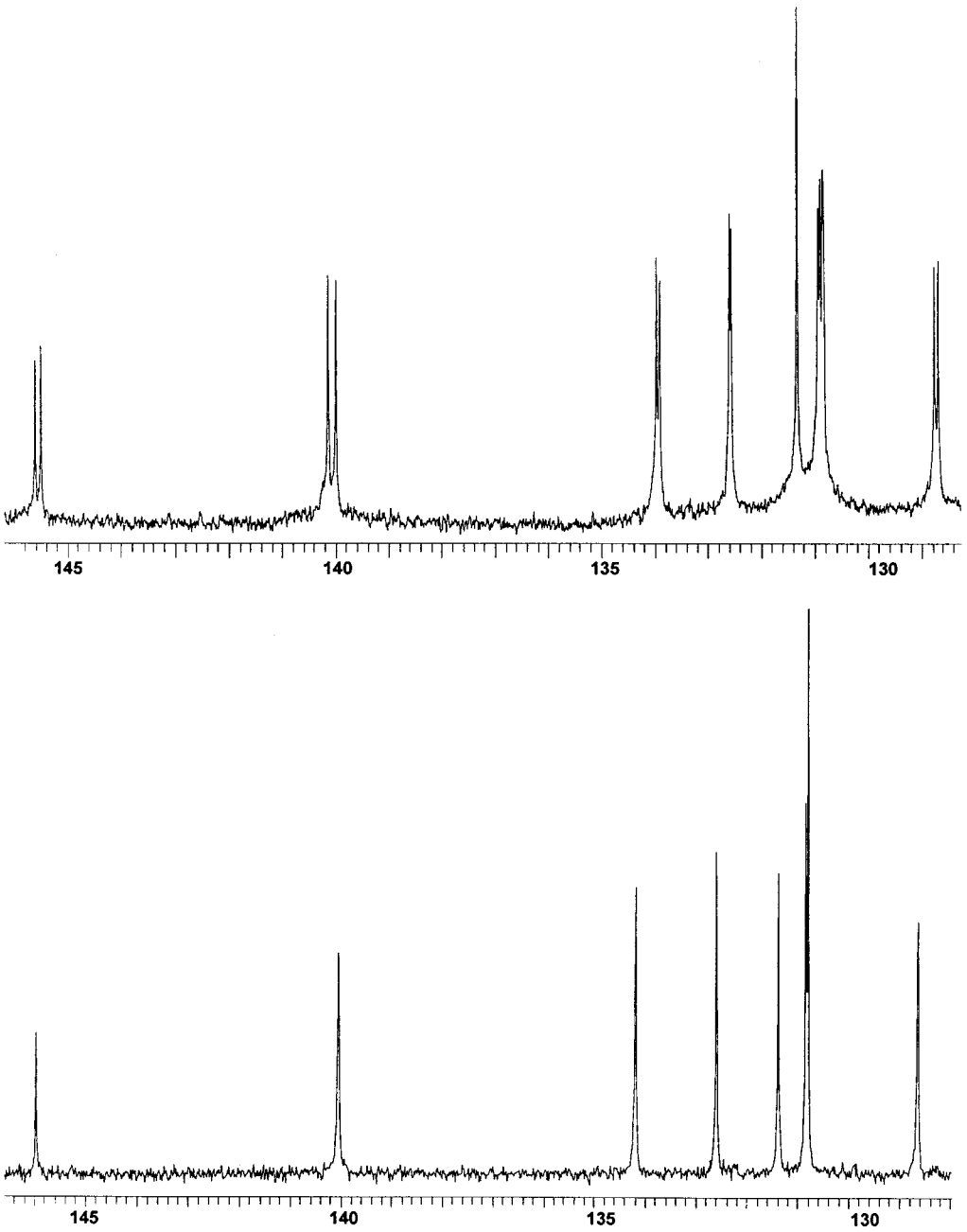

Figure 3. ^{13}C NMR spectra of the olefinic region of **2** in THF-d_8 at 232 K (top) and ambient temperature (bottom). The doublets in the top spectrum correspond to the meso and racemic isomers, which are observed when RI is slow on the NMR time scale.

Table 2. Torsional Angles and Relative Energies for HF/6-31G* Geometry-Optimized Conformers of *meso*- and *rac*-1

conformer	$\omega(C_1{=}C_2)^a$	$\omega(C_{1'}{=}C_{2'})^a$	$(E_{MP2})_{rel}{}^{b,c}$	$(E_{HF} + ZPE)_{rel}{}^{b,d}$	$(E_{MP2} - E_{HF})_{rel}{}^{e}$
meso-AA	2.8	35.9	1.63	2.15	−0.67
meso-AB′	3.5	7.0	0	0	0
meso-AC	17.8	13.4	1.05	1.27	−0.32
meso-A′C	18.5	19.1	1.44	1.15	0.22
rac-AA′	7.5	40.9	2.14	2.09	−0.10
rac-AB	2.6	2.6	0.61	0.65	−0.12
rac-A′B′	9.0	9.0	0.67	0.29	0.38
rac-AC	13.0	19.6	0.97	1.17	−0.28
rac-A′C	18.4	19.8	1.35	1.12	0.14

[a] In deg. [b] $E - E_{meso-AB'}$; in kcal mol^{-1}. [c] MP2/6-31G*//HF/6-31G*. [d] HF/6-31G*//HF/6-31G*. ZPEs were scaled by a factor of 0.9135: Scott, A. P.; Radom, L. *J. Phys. Chem.* **1996**, *100*, 16502. [e] [E(MP2/6-31G*//HF/6-31G*) − E(HF/6-31G*//HF/6-31G*)] − [$E_{meso-AB'}$(MP2/6-31G*//HF/6-31G*) − $E_{meso-AB'}$(HF/6-31G*//HF/6-31G*)]; in kcal mol^{-1}.

In AC-type conformers, one C_1C_2 double bond is within 10−21° of being eclipsed with CH_A while the other is similarly oriented with regard to the CC bond between the bridge atom and C_1 of the other COT ring. These conformers are less stable in **1** than the AB-type owing to a close contact between H_2 of the C ring and C_1 of the

Table 3. Torsional Angles and Relative Energies for HF/6-31G* Geometry-Optimized Conformers of *meso*- and *rac*-2

conformer	$\omega(C_1{=}C_2)^a$	$\omega(C_{1'}{=}C_{2'})^a$	$(E_{MP2})_{rel}{}^{b,c}$	$(E_{HF}+ZPE)_{rel}{}^{d,e}$	$(E_{MP2}-E_{HF})_{ref}{}^f$
meso-AA	2.2	23.3	1.36	1.95	−0.43
meso-AB′	6.2	1.5	0	0.18	0
meso-AC	15.8	10.6	0.37	0.74	−0.26
meso-A′C	9.2	21.2	0.57	0.43	0.25
rac-AA′	12.2	8.0	0.91	1.25	−0.11
rac-AB	2.6	2.6	1.12	1.40	−0.10
rac-A′B′	1.8	1.8	0.17	0	0.29
rac-AC	13.3	16.3	0.38	0.61	−0.06
rac-A′C	10.5	18.1	0.70	0.51	0.22

[a] In deg. [b] $E - E_{meso-AB'}$; in kcal mol^{-1}. [c] MP2/6-31G*//HF/6-31G*. [d] $E - E_{rac-A'B'}$. [e] HF/6-31G*//HF/6-31G*. ZPEs were scaled by a factor of 0.9135; see footnote d, Table 2. [f] [E(MP2/6-31G*//HF/6-31G*) − E(HF/6-31G*//HF/6-31G*)] − [$E_{rac-A'B'}$(MP2/6-31G*//HF/6-31G*) − $E_{rac-A'B'}$(HF/6-31G*//HF/6-31G*)]; in kcal mol^{-1}.

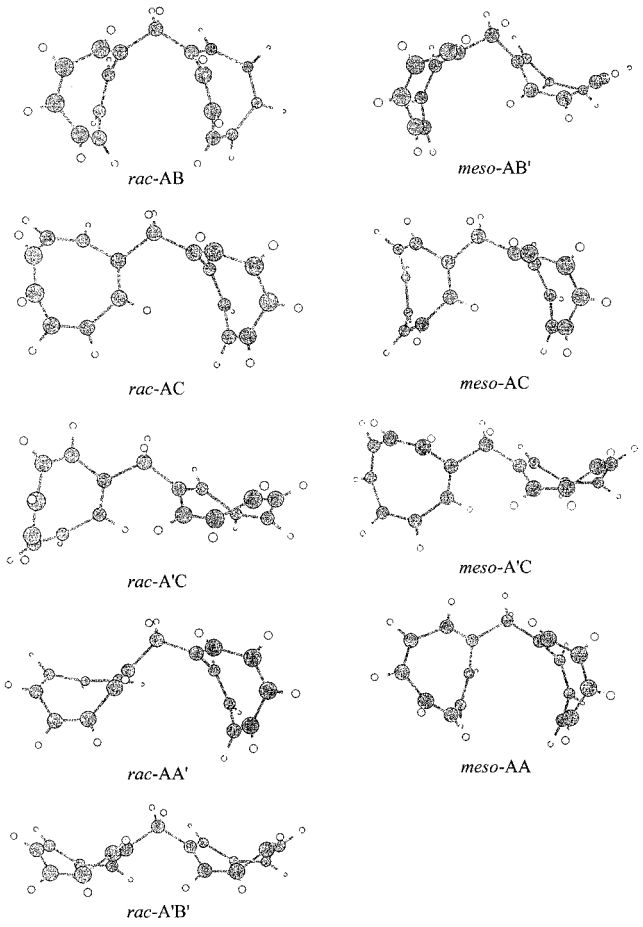

Figure 4. Geometry-optimized structures of stable conformers of *rac*-**1** (left) and *meso*-**1** (right) calculated at HF/6-31G*.

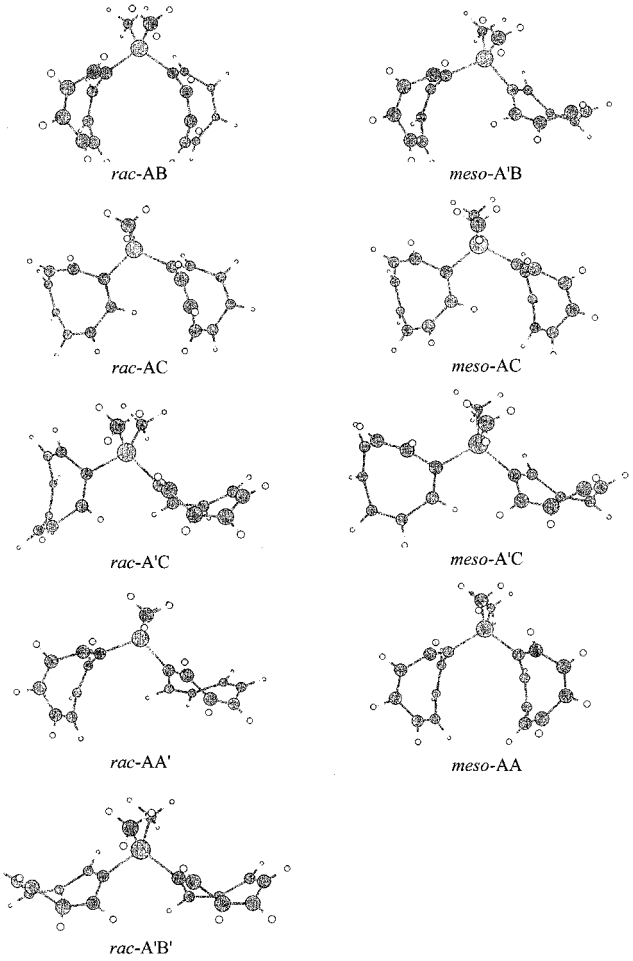

Figure 5. Geometry-optimized structures of stable conformers of *rac*-**2** (left) and *meso*-**2** (right) calculated at HF/6-31G*.

A ring. However, the latter interaction is reduced in **2** owing to greater separation of the rings as a result of C−Si bonds being longer than C−C bonds. Consequently, AC-type conformers are relatively more stable in **2**.

Finally, in the AA-type conformers, one CC double bond is nearly eclipsed with CH_A while the other is either in a similar position (as in **2**) or in a more nearly staggered conformation but closest to CH_A, as in **1**. These are the least stable conformers in **1** since inter-ring H···H or H···C repulsions are encountered if both double bonds are nearly eclipsed with CH_A, but these interactions are attenuated somewhat in **2**. We were not able to locate a minimum for *meso*-A′A′ of **1** or **2**.

In the right-hand columns of Tables 2 and 3 we list the changes in relative energies of the conformers of **1** and **2**, respectively, on going from HF/6-31G* to MP2/6-31G*, both at the HF/6-31G*-optimized geometry. These changes are given relative to that for *meso*-AB′. This is the most appropriate reference, not only because it is the most stable conformer (except for **2** at E_{HF}+ZPE, Table 3) but also because it has one ring endo and one ring exo and therefore is at a conformational "middle ground".

There are three conformers whose values of $(E_{MP2}-E_{HF})_{rel}$ are positive. In each of these one ring is exo and the other is either completely (*rac*-A′B′) or largely exo (*rac*-A′C and *meso*-A′C). Five conformers have negative $(E_{MP2}-E_{HF})_{rel}$ values. Of these, the largest negative values are where the two rings are either endo to each other (i.e., face-to-face) (*meso*-AA) or offset face-to-face (*rac*-AB). The remaining three have one ring endo and the second

ring either exo (*rac*-AA′) or largely exo (*rac*-AC and *meso*-AC).

The $(E_{MP2}-E_{HF})_{rel}$ values can be understood as follows. Dynamic electron correlation affects the conformers of **1** and **2** differently primarily as a result of inter-ring contributions, which are most important for the π electrons. Thus, the greatest effect is expected to occur in the more face-to-face conformations, where inter-ring π/π overlap is greatest (Figures 4 and 5). This interpretation is supported by the observation that the signs and magnitudes (to within ±0.2 kcal mol^{-1}) of ΔE_{rel} for almost all of the conformers of **1** are the same on going from the 3-21G basis set (with structures optimized at HF/3-21G) to the more flexible (and therefore "longer range") 6-31G* basis set as for the corresponding $(E_{MP2}-E_{HF})_{rel}$ values in Tables 2 and 3.

Analysis of the $(E_{MP2}-E_{HF})_{rel}$ values for **1** in Table 2 leads to the conclusion that correlation energy increases in the order exo ring (A′ or B′) < C ring < endo ring (A or B) and AB < AC (or AC′) < AA. That is, *the closer the π bonds of the two rings are to each other, the greater the correction for dynamic electron correlation*. Similar effects can be seen for **2** at the extremes, i.e., *meso*-AA and *rac*-A′B′ are respectively the most and least stabilized by electron correlation (Table 3).

Relative Energies of Diastereomers. Since the lowest energy meso conformer of **1** (*meso*-AB′) is calculated to be 0.6 kcal mol^{-1} more stable than the lowest energy racemic conformer (*rac*-AB) at MP2/6-31G*//HF/6-31G* (Table 2), it may at first appear that these calculations do not reproduce the value of 0.1 kcal mol^{-1} measured for $\Delta G°_{isom}$ at 229 K. However, when the vibrational zero point energy (ZPE), conformational enthalpy (H_{conf}), entropy of mixing of conformers and their enantiomers (S_{mix}) and the entropy due to the symmetry number (σ) are considered according to eqs 1−5,[27] the free energy of the meso isomer is calculated to be only 0.09 kcal mol^{-1} less than that of the racemic isomer at 229 K (Table 4). This is in excellent agreement with the measured value of ΔG_{isom} *if meso*-**1** is the more stable isomer.

$$G_{rel} = E_{rel} + G_{conf} \quad (1)$$

$$G_{conf} = H_{conf} - T(S_{mix} + S_{sym}) \quad (2)$$

$$H_{conf} = \sum_i n_i H_i \quad (3)$$

$$S_{mix} = -R \sum_i n_i \ln n_i + n_i R \ln 2 \quad (4)$$

$$S_{sym} = -R \ln \sigma \quad (5)$$

The elements of these calculations and several potential complications are as follows. All of the racemic conformers exist as enantiomeric pairs. This contributes $n_i R \ln 2$ to S_{mix}, where n_i is the mole fraction of conformer i and R is the gas constant. *Rac*-AB and *rac*-A′B′ can only interconvert between enantiomers via two ring inversions. However, these conformers have a 2-fold axis of symmetry and a symmetry number of 2, which contributes $-n_i R \ln 2$ to the entropy and cancels S_{mix} due to enantiomers. Although the other three racemic conformers do not have a 2-fold axis, each of them can interconvert between enantiomers (e.g., *rac*-AC = *rac*-CA) via a facile 1/3 rotation of each COT ring giving them an *effective* σ of 2.

Similarly, each meso *conformer* (as opposed to the meso *diastereomer*) is chiral and therefore exists as a pair of enantiomers. However, as with the racemic conformers, these are readily interconverted by 1/3 rotations (ca. 30° rotations in the case of *meso*-AA) of the COT rings giving an effective σ of 2 and canceling S_{mix} due to enantiomers. Instead, the low-energy torsions that interconvert enantiomers will contribute to the vibrational entropy. Since this approach treats the two diastereomers in the same manner, any deficiencies in the treatment should tend to cancel when comparing the meso and racemic isomers.

The corresponding calculations for *meso*- and *rac*-**2** are also given in Table 4. G_{rel} is calculated to be 0.14 kcal mol^{-1} in favor of the *racemic isomer*, a value that suggests, contrary to experiment, a larger energy difference between the two diastereomers for **2** than for **1**. Consequently, the agreement of G_{rel} with $\Delta G°_{isom}$ for the latter compound is probably fortuitious.

Calculation of G_{rel} using the relative MP2 energies in Tables 2 and 3 gave values in favor of the meso isomer of 0.25 and 0.06 kcal mol^{-1} for **1** and **2**, respectively. These calculations place the racemic isomer about 0.1 kcal mol^{-1} too high relative to the meso isomer but, unlike the $(E_{HF} + ZPE)_{rel}$ calculations, correctly show a greater difference for **1**. The relatively large differential effects of dynamic electron correlation reported in Tables

Table 4. Relative Thermodynamic Parameters for *Meso*- and *Rac*-1 and 2 at 229 K[a]

compound	isomer	H_{conf}[b,c]	S_{conf}[c,d]	G_{conf}[b]	G_{rel}[b]
1	meso	0.16	1.00	−0.06	0
	racemic	0.26	2.27	−0.26	0.09
2	meso	0.18	2.06	−0.29	0
	racemic	0.28	2.25	−0.24	−0.14

[a] These calculations employed eq 1−5. [b] In kcal mol^{-1}. [c] Mole fractions were calculated from $\Delta(E_{HF} + ZPE)_{rel}$ (Tables 2 and 3) using eq 10.2 in ref 27. [d] In cal mol^{-1} K^{-1}.

Table 5. Kinetic Data for Ring Inversion and Bond Shift in 1 and 2 in THF-d_8

compound	process[a]	T (K)	k (s^{-1})	T (K)	$\Delta G^{‡}$[b]
1 (major isomer)	RI[c]	230−272	52	272	13.7
			7.7	240	13.0
	RI	230−240	7.4	240	13.0
	BS[d,e]	272−298	1.9	272	15.5
			96[f]	306	15.1
1 (minor isomer)	RI[c]	230−272	69	272	13.6
			9.6	240	12.9
	RI	230−240	9.5	240	12.9
	BS[d,e]	272−298	1.9	272	15.5
			96[f]	306	15.1
2	RI[c]	260−296	12	272	14.5
			5.0	260	14.3
			115[g]	306	15.0
	RI	250−260	4.8	260	14.3
	BS[e]	303−312	8.8	306	16.6
			0.12[h]	272	17.0

[a] From ^{13}C line widths unless indicated otherwise. [b] In kcal mol^{-1}; ±0.1. [c] From ^{13}C line shape analysis. [d] Weighted average for the two diastereomers. [e] Ref 5. [f] Extrapolated using $\ln(k/T) = 29.52 - 9.388 \times 10^3\ T^{-1}$. [g] Extrapolated using $\ln(k/T) = 16.01 - 5.198 \times 10^3\ T^{-1}$. [h] Extrapolated using $\ln(k/T) = 29.73 - 1.020 \times 10^4\ T^{-1}$.

(27) Eliel, E. L.; Wilen, S. H.; Mander, L. N. *Stereochemistry of Organic Compounds*; Wiley: New York, 1994; pp 629−34.

Table 6. Activation Energies for Ring Inversion in 1 and 2 Calculated for Structures Optimized at HF/6-31G*[a]

compd	TS conformer[b]	$\Delta E^{\ddagger}_{MP2}$[c]	$\Delta(E^{\ddagger}_{HF} + ZPE)$[c]
1	AB	16.4	15.8
	AB′	16.7	15.9
2	AB′	18.0	17.0[d]
	AB	18.1	17.4[d]

[a] Relative to *meso*-AB′ ground state unless indicated otherwise. [b] The first letter refers to the planar ring. [c] In kcal mol^{-1}. [d] Relative to *rac*-A′B′ ground state.

2 and 3 suggest that it is important to incorporate correlation, even at the level of approximation employed in MP2. It is possible that geometry optimizations at MP2/6-31G* would show still better agreement with experiment, but these calculations are too large to be performed at present.

We also calculated MM2-optimized structures for the conformers of **1** and **2**. Calculation of G_{rel} as in Table 4 using the MM2 energies gave values of 0.35 kcal mol^{-1} in favor of the meso isomer for **1** and 0.51 kcal mol^{-1} in favor of the racemic isomer for **2**. Both values, especially the latter, disagree with the experimental values of $\Delta G°_{isom}$. Furthermore, the most stable conformers calculated by MM2 are *meso*-AA for **1** and *rac*-AB for **2**, which are the least and next-to-least stable conformers, respectively, at HF/6-31G*. These results indicate that the latter is a more reliable model for **1** and **2** than MM2 as parametrized in CHEM3D owing to a better treatment of inter-ring interactions.

Kinetics of Ring Inversion. The rate constant for RI can be calculated from k_{1exch} by employing eq 6.[17] The

$$k_{1exch} = 2[k_{RI} + (k_{BS}/2)] \qquad (6)$$

factor of 2 in front of the brackets is required because inversion of either of the COT rings in **1** or **2** results in an exchange of diastereomers. The value of k_{BS} was obtained from the rate of pairwise exchange of C_2, C_3 and C_4 with C_6, C_7 and C_8, respectively.[5] The denominator of $k_{BS}/2$ reflects the fact that each BS results in inversion one-half of the time.

Kinetic data for RI and BS in **1** and **2** are given in Table 6. The values of $\Delta G^{\ddagger}_{BS}$ at 298 K (15.3 and 16.7 kcal mol^{-1}, respectively) are similar to those for methylCOT and trimethylsilylCOT (15.6 and 16.4 kcal mol^{-1}, respectively).[20] The small difference in $\Delta\Delta G^{\ddagger}_{BS}$ for the two pairs of compounds (1.4 vs 0.8 kcal mol^{-1}, respectively) might reflect greater steric repulsions in the GS of **1** vs methylCOT and greater van der Waals attractions in the GS of **2** relative to trimethylsilylCOT, although TS effects also need to be considered. We plan to explore this issue in greater depth.

We are primarily interested in the difference between $\Delta G^{\ddagger}_{BS}$(**2**) − $\Delta G^{\ddagger}_{BS}$(**1**) and $\Delta G^{\ddagger}_{RI}$(**2**) − $\Delta G^{\ddagger}_{RI}$(**1**) ($\Delta\Delta G^{\ddagger}_{BS}$ − $\Delta\Delta G^{\ddagger}_{RI}$). Kinetic data are compared at 272 K since three of the four required data points (k_{RI} for **1** and **2** and k_{BS} for **1**) were measured at this temperature. Because RI is fast on the NMR time scale at the temperatures at which we studied BS, k_{BS}(**1**) is the weighted average for the major and minor isomers. Consequently, we also employed the weighted average of k_{RI} (60 s^{-1}) in this comparison based on the reasonable assumption that the ratio of diastereomers obtained at 229, 240 and 263 K also applies at 272 K. Further, because the value of k_{BS}(**2**) at 272 K involves an extrapolation from a rather limited temperature range (303−312 K), we also extrapolated k_{BS}(**1**), which was determined over a much larger range (272−298 K), to 306 K. This gave a value of $\Delta\Delta G^{\ddagger}_{BS}$ of 1.5 kcal mol^{-1}, in agreement with the difference obtained at 272 K.

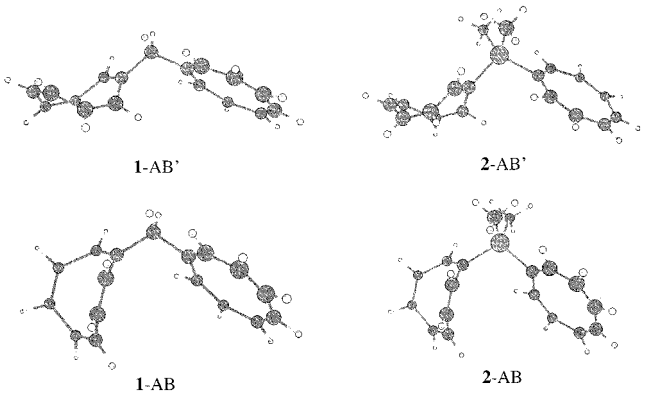

Figure 6. Geometry-optimized transition structures for ring inversion in **1** (left) and **2** (right) calculated at HF/6-31G*. The first letter refers to the planar ring.

Interestingly, $\Delta\Delta G^{\ddagger}_{BS}$ is 0.6$_5$ kcal mol^{-1} greater than $\Delta\Delta G^{\ddagger}_{RI}$ at 272 K. The uncertainty in the latter is ±0.2 kcal mol^{-1}, whereas that of $\Delta\Delta G^{\ddagger}_{BS}$ is a bit larger owing to the extrapolation of k_{BS}(**2**). Consequently, the increase in the differential substituent effect of CH_2 vs $Si(CH_3)_2$ for BS relative to RI is comparable to the combined experimental uncertainties. Since both RI and BS originate from the same GS, *any differential substituent effect must be operative in the TS*. Further, the substituents must influence BS in a way other than through the steric and σ hybridization effects that have been discussed for RI. Additional work is required in order to fully understand the effects of donors and acceptors on π bond shift in COT, especially considering a possible role for heavy-atom tunneling in this process.[28]

We also optimized the geometries for the RI TSs of **1** and **2** at HF/6-31G* (Figure 6) and calculated the activation energies [$\Delta E^{\ddagger}_{MP2}$ and $\Delta(E^{\ddagger}_{HF}$+ZPE)] from the difference in total energies of the lowest-energy ground and transition conformers (Table 6). Both calculated values of $\Delta E^{\ddagger}$ are too large, more so for $\Delta E^{\ddagger}_{MP2}$ than for $\Delta(E^{\ddagger}_{HF} + ZPE)$. Further, the calculated value of $\Delta E^{\ddagger}_{RI}$(**2**) − $\Delta E^{\ddagger}_{RI}$(**1**) is closer to the experimental difference ($\Delta\Delta G^{\ddagger}_{RI}$ = 1.0 kcal mol^{-1} at 272 K) for E_{HF} + ZPE (1.2 kcal mol^{-1}) than for E_{MP2} (1.6 kcal mol^{-1}).

Summary

Ground state and ring inversion transition state conformations of **1** and **2** have been optimized by ab initio molecular orbital theory at the HF/6-31G* level, and their energies have been calculated at MP2/6-31G*. Analysis of four meso and five racemic conformers of **1** and **2** has elucidated the contributions of torsional strain, steric interactions and dynamic electron correlation. Calculations of the meso:racemic ratio using the MP2/6-31G* energies of the conformers optimized at HF/6-31G* and corrected for conformational enthalpy and entropy con-

(28) (a) Carpenter, B. K. *J. Am. Chem. Soc.* **1983**, *105*, 1700. (b) Dewar, M. J. S.; Merz, K. M., Jr. *J. Phys. Chem.* **1985**, *89*, 4739. (c) Andrés, J. L.; Castaño, O.; Morealle, A.; Palmeiro, R.; Gomperts, R. *J. Chem. Phys.* **1998**, *108*, 203.

tributions afforded values in good agreement with experiment *if* the meso isomer is the major diastereomer of **1**.

Measurement of the rate constants for RI by dynamic NMR spectrometry showed that **1** reacts five times faster than **2** at 272 K. The corresponding ratio for bond shift (16) is three times larger, suggesting that substituent effects not present in the RI TS are operative in the BS TS.

Experimental Section

General. Compounds **1** and **2** were synthesized by Dr. Patrik Boman[2,5] by the method of Echegoyen et al.[26] ^{1}H and ^{13}C NMR spectra were recorded with a Bruker AMX2-400 instrument. The temperature was measured with a methanol sample before or after each experiment.[29] As reported earlier,[2] heating due to ^{13}C homodecoupling was assumed to be negligible and a maximum error of ±1 °C was estimated in the measured temperatures. All experiments were performed at least twice on each sample. Molecular orbital calculations were performed with Spartan 4.1[30] and Gaussian 98W[31] software using the 3-21G,[32] 3-21G$^{(*)}$[33] and 6-31G*[34] basis sets. The RI TS geometries were optimized by constraining the CCCC dihedral angles of one ring to 0°. Ground-state energy minima and ring inversion transition states were confirmed by analytical frequency analysis, which showed zero and one imaginary frequencies, respectively. Molecular mechanics calculations were performed with the MM2[35] program in CHEM3D Pro 5.0.[36]

Kinetics. Rate constants were determined by ^{13}C line shape analysis using the program gNMR 4.0.1.[37] The chemical shifts, intrinsic line widths and ratios of diastereomers were employed as input constants for the calculation of rate constants. Chemical shifts above the coalescence temperature were obtained by a linear least-squares fit of the values below coalescence. The line widths of the nonexchanging carbons C_1 and C_5 of the COT rings were used for the intrinsic line widths of the olefinic carbons, whereas those for the methylene and methyl carbons in the isomers of **1** and **2**, respectively, were determined from the low-temperature spectra and assumed to remain constant over the experimental temperature range. Similarly, diastereomeric ratios were obtained by integration of the ^{1}H signals at low temperature and assumed to remain constant over the experimental temperature range. The peaks (−44 °C) at δ 46.87 and 47.42 (CH_2) and δ 134.72, 134.88, 142.18 and 142.25 (olefinic) were employed for line shape analysis for **1**, whereas those (−58 °C) at δ −5.36, −4.98 and −4.80 (CH_3) and δ 139.99, 140.14, 145.51 and 145.62 (olefinic) were used for **2**. At some temperatures (see Table 5), k_{1exch} and k_{-1exch} could also be determined from the exchange broadening of the above ^{13}C peaks using the equation $k_{1exch} = \pi\Delta w_{exch}$, where Δw_{exch} is the peak (width at half-height) broadening due to exchange.[38] The protocol for these measurements has been presented previously.[3,5]

Acknowledgment. We thank the Intel Corporation for the donation of a computer to Carnegie Mellon University, the Carnegie Mellon SURG program and the Arnold and Mabel Beckman Foundation for a Beckman Scholars Program Grant to S.A.V.

JO001793A

(29) Van Geet, A. L. *Anal. Chem.* **1970**, *42*, 679.
(30) Spartan 5.1; Wavefunction, Inc.: 18401 Von Karman Ave., Suite 370, Irvine, CA 92612.
(31) Gaussian 98, Revision A.6; Frisch, M. J.; Trucks, G. W.; Schlegel, H. B.; Scuseria, G. E.; Robb, M. A.; Cheeseman, J. R.; Zakrzewski, V. G.; Montgomery, J. A., Jr.; Stratmann, R. E.; Burant, J. C.; Dapprich, S.; Millam, J. M.; Daniels, A. D.; Kudin, K. N.; Strain, M. C.; Farkas, O.; Tomasi, J.; Barone, V.; Cossi, M.; Cammi, R.; Mennucci, B.; Pomelli, C.; Adamo, C.; Clifford, S.; Ochterski, J.; Petersson, G. A.; Ayala, P. Y.; Cui, Q.; Morokuma, K.; Malick, D. K.; Rabuck, A. D.; Raghavachari, K.; Foresman, J. B.; Cioslowski, J.; Ortiz, J. V.; Stefanov, B. B.; Liu, G.; Liashenko, A.; Piskorz, P.; Komaromi, I.; Gomperts, R.; Martin, R. L.; Fox, D. J.; Keith, T.; Al-Laham, M. A.; Peng, C. Y.; Nanayakkara, A.; Gonzalez, C.; Challacombe, M.; Gill, P. M. W.; Johnson, B.; Chen, W.; Wong, M. W.; Andres, J. L.; Gonzalez, C.; Head-Gordon, M.; Replogle, E. S.; Pople, J. A. Gaussian, Inc.: Pittsburgh, PA, 1998.
(32) Pietro, W. J.; Francl, M. M.; Hehre, W. J.; DeFrees, D. J.; Pople, J. A.; Binkley, J. S. *J. Am. Chem. Soc.* **1982**, *104*, 5039.
(33) Dobbs, K. D.; Hehre, W. J. *J. Comput. Chem.* **1986**, *7*, 359.
(34) Hehre, W. J.; Ditchfield, R.; Pople, J. A. *J. Chem. Phys.* **1972**, *56*, 2257.
(35) (a) Burkert, U.; Allinger, N. L. *Molecular Mechanics*, ACS Monograph No. 177, American Chemical Society: Washington, DC, 1982; p 339. (b) Allinger, N. L. *J. Am. Chem. Soc.* **1977**, *99*, 8127.
(36) CHEM3D Pro 5.0; Cambridge Soft Corp.: Cambridge, MA 02140-2317.
(37) gNMR 4.0.1; Cherwell Scientific Publishing: The Magdalen Centre, Oxford Science Park, Oxford OX4 4GA, U.K.
(38) Sandström, J. *Dynamic NMR Spectroscopy*; Academic Press: London, 1982; pp 14−18.